doi:10.14311/ppt.2024.2.39
Plasma Physics and Technology **11**(2):39–44, 2024

STUDY OF HIGH–FREQUENCY ELECTRODELESS MERCURY CAPILLARY DISCHARGE IN THE MAGNETIC FIELD

N. Zorina[a,*], G. Revalde[a,b], A. Abola[a], A. Skudra[a], R. Gudermanis[a]

[a] *Institute of Atomic Physics and Spectroscopy, University of Latvia, Jelgavas str. 3, LV–1004, Riga, Latvia*
[b] *Institute of Technical Physics, Riga Technical University, P. Valdena str. 7, LV–1048, Riga, Latvia*
[*] natalja.zorina@lu.lv

Abstract. We analyzed shapes of Hg 253.7 nm spectral line, emitted from a micro–size electrodeless Hg/Xe capillary lamp in a magnetic field for its usage in Zeeman atomic absorption spectrometry. Measurements for several different lamp positions were conducted. Obtained profiles were presented as a Fredholm integral equation of the first kind and separated from an instrumental function. The gas temperature, the dependence of Zeeman splitting on the intensity of the magnetic field, and the magnetic field's exact value in the experiment were determined.

Keywords: high–frequency electrodeless lamp, ill–posed inverse task, Zeeman effect, mercury isotope, deconvolution, Zeeman atomic absorption spectrometry.

1. Introduction

A light source with extremely narrow spectral lines is required for use in high–precision atomic absorption spectrometry (AAS). One solution is to use a capillary low–temperature low–pressure electrodeless discharge to receive optically thin radiation. Furthermore, in the case of such elements as mercury, arsenic, selenium, etc., high–frequency low–temperature low–pressure electrodeless lamps (HFEDLs) offer significantly higher intensities, better stability, and longer lifetimes than hollow cathode lamps [1]. Zeeman AAS (ZAAS) with HFEDLs is one of the most sensitive methods for detecting heavy metals in the environment in low concentrations [2]. For this method resonance spectral lines in the UV spectral range are used. In the case of mercury 253.7 nm line is exploited.

However, micro–size discharge in UV spectroscopic diagnostics is also a challenge due to the very small dimensions and weak intensity. In addition, the optical properties of such capillary discharge lamps depend largely on the operation positions [3].

This paper focuses on analyzing the emission spectral line shapes of mercury capillary lamp in a magnetic field at a wavelength of 253.7 nm in dependence on working positions: the lamp is situated horizontally, vertically with reservoir up and vertically with reservoir down. The aim is to find out experimentally which of the three operating positions is the most suitable for use in ZAAS.

In our prior investigation [4] only the visible triplet of mercury was measured.

2. Experiment

Mercury isotope capillary high–frequency electrodeless light sources were prepared in our laboratory at the Institute of Atomic Physics and Spectroscopy for their use in ZAAS. Lamps consist of a spherical part (diameter of 10 mm) with a long cylindrical capillary tail. The capillary discharge radius was 500 μm, and the length was about 20 mm. An example of the Hg light source used in this study can be seen in Figure 1.

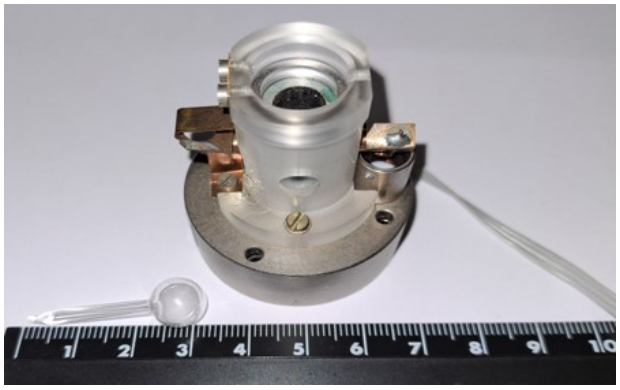

Figure 1. The Hg light source and the excitation generator.

The light sources were filled with a stable ^{198}Hg isotope with 98% saturation and Xe as a buffer gas. The pressure of Xe in the lamps was 2 Torr ($\approx$ 267 Pa).

The capacitatively coupled discharge was excited with outer electrodes. The plasma was excited by placing the lamp in the electromagnetic field of 100 MHz frequency. In addition, to use the lamps in ZAAS, magnetic field was applied.

Spectral line shapes of the 253.7 nm resonance line emitted from the mercury capillary light sources were measured by the Fourier spectrometer Bruker IFS HR125 with a spectral resolution of 0.015 cm^{-1}.

The cold spot temperature of the lamp was measured by the thermal infrared camera (FLIR E75) in three different lamp positions.

3. Theoretical background

3.1. Deconvolution of spectral line profiles

Reconstruction of the real line shape from the measured one is so–called inverse ill–posed task because small uncertainties in a measurement give large deviations in a solution. It can be described by the Fredholm integral equation of the first kind [4]:

$$\int_a^b A(\nu,\nu')y(\nu')\mathrm{d}\nu = f(\nu),\ c \le \nu \le d, \qquad (1)$$

here A – instrument function, y – real profile, f – measured profile, a, b, and c, d are the limits of real and measured (experimental) profiles accordingly.

Since it is a complicated task, sometimes the instrument function is neglected. In general, it is acceptable for high temperatures and dense plasmas [5, 6]. However, in the case of low–pressure plasma, the instrument function is of the same order as the experimental profile, and it can cover the detailed structure of the spectral line. In this paper, the reconstruction of the real line shape is implemented by a method developed before [7]. Using this method instead of the initial ill–posed problem, we get a well–posed task, which is described by the Fredholm integral equation of the second kind:

$$\alpha(y_\alpha(t) - q y''_\alpha(t)) + \int_a^b k(t,\nu')y_\alpha(\nu')\mathrm{d}\nu' = F(t), \quad (2)$$

where: $t \in [a,b]$,
$k(t,\nu') = k(\nu',t) = \int_c^d \tilde{A}(\nu,t)\tilde{A}(\nu,\nu')\mathrm{d}\nu$,
$F(t) = \int_c^d \tilde{A}(\nu,t)\tilde{f}(\nu)\mathrm{d}\nu$.

Equation (2) can be solved using classical methods. Here α is the regularization parameter, which establishes the correspondence between the requirement of the stability of the solution and its reliability. In this work, the regularization parameter was obtained using the discrepancy minimization method. The initial value of α for the further solution was chosen according to the selection method [4].

3.2. Hyperfine splitting of mercury 253.7 nm line due to the Zeeman effect

When HFEDL is filled with natural mercury, the resonance line is very broad (total width is around 1.1 – 1.2 cm^{-1}).

In Figure 2 we can see an example of the Hg 253.7 nm spectral line (natural isotope mixture) in an electromagnetic field of 100 MHz frequency [8]. All stable mercury isotopes are marked.

The structure of Hg profiles becomes more complicated due to the splitting into Zeeman sublevels and the formation of the hyperfine structure in the magnetic field.

Five mercury bosons have zero nuclear spin $I = 0$ and three Zeeman sublevels, which are characterized by quantum number m ($m = 0, \pm 1$). Two fermions have non–zero nuclear spin.

The ^{201}Hg isotope is a fermion with non–zero nuclear spin $I = 3/2$. Using the formula for values of full moment $F(F = J + I)$ [9]:

$$F = I + J, I + J - 1, \ldots |I - J|, \qquad (3)$$

we get the hyperfine splitting of the $^3P_1$ state into three states ($F = 5/2, 3/2, 1/2$).

We measured the $F = 3/2 \to F' = 5/2$ transition.

The splitting of ground state $^1S_0$ ($F = 3/2$) in a weak magnetic field is negligible [10, 11] as the nuclear Landé factor is much smaller than the orbital and the electron ones (by the electron–to–proton mass ratio). But the quantum number m_F has $2\ F\ +\ 1$ values [9]. Therefore the excited state $^3P_1$, $F = 5/2$ splits into six Zeeman sublevels: $-5/2; -3/2; -1/2; 1/2; 3/2; 5/2$, characterized by magnetic quantum number m_F.

Similarly, can be found the splitting into Zeeman sublevels for another fermion: ^{199}Hg. In this case, $I = 1/2$ sequentially leads to hyperfine splitting of the $^3P_1$ state into two states characterized by $F = 3/2$ and $F = 1/2$. Thus, considering that m_J has $2J + 1$ values [12], state $^3P_1(F = 3/2)$ splits into four Zeeman sublevels: $-3/2; -1/2; 1/2; 3/2$, characterized by magnetic quantum number m_F in case of ^{199}Hg.

The magnetic interaction energy in a weak external field in the case of fermions can be described by the following equation:

$$\Delta W_{FH} = \mu_B H_0 m_F g_F, \qquad (4)$$

where Landé factor g_F for fermions is described by the following equation [9]:

$$g_F \approx g_J \frac{F(F+1) + J(J+1) - I(I+1)}{2F(F+1)}. \qquad (5)$$

In the case of bosons equation (4) can be written in the form [12]:

$$\Delta W_{FH} = \mu_B H_0 m_J g_J, \qquad (6)$$

where Landé factor g_J for bosons is:

$$g_J = 1 + \frac{J(J+1) + S(S+1) - L(L+1)}{2J(J+1)}. \qquad (7)$$

For fermions as well as for bosons:
H_0 – external magnetic field,
m_F and m_J – magnetic quantum numbers,
$\mu_B = \frac{e\hbar}{2m_e}$ – Bohr magneton.

Taking into account elementary charge e, reduced Plank constant $\hbar$ and electron mass m_e, following value of Bohr magneton is obtained:
$\mu_B \approx 5.7 \times 10^{-5}\, eV/T \approx 4.7 \times 10^{-5}\, \mathrm{cm}^{-1} Oe^{-1}$.

4. Results and discussions

4.1. Deconvolution and calculation of temperature

In Figure 3 we can see the example of the shapes of the emitted Hg 253.7 nm line, depending on the position of the lamp in a magnetic field.

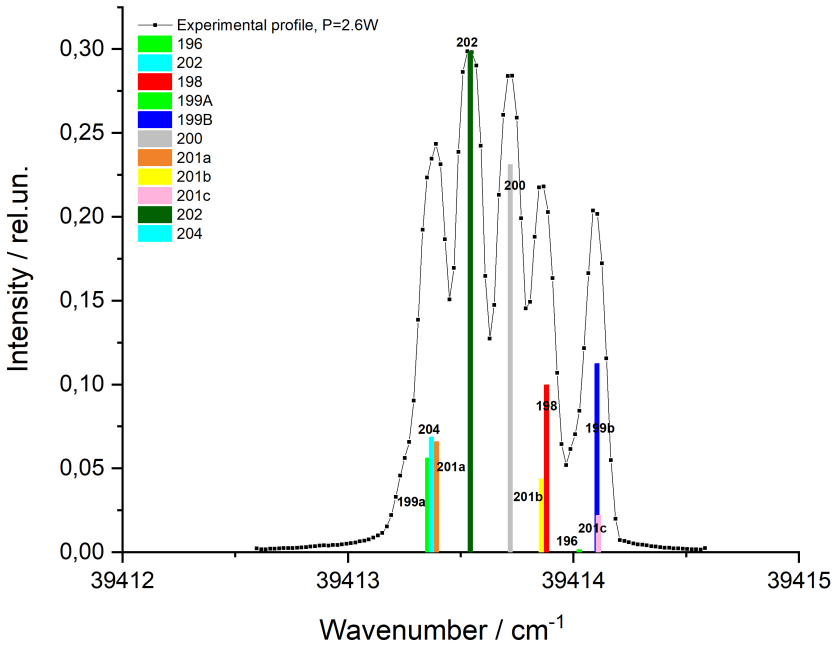

Figure 2. The profile emitted from HFEDL filled with natural isotope mixture (was measured at an excitation generator power value of 2.6 W). The line strengths of the markers of the isotopes are normalized to the ^{198}Hg isotope.

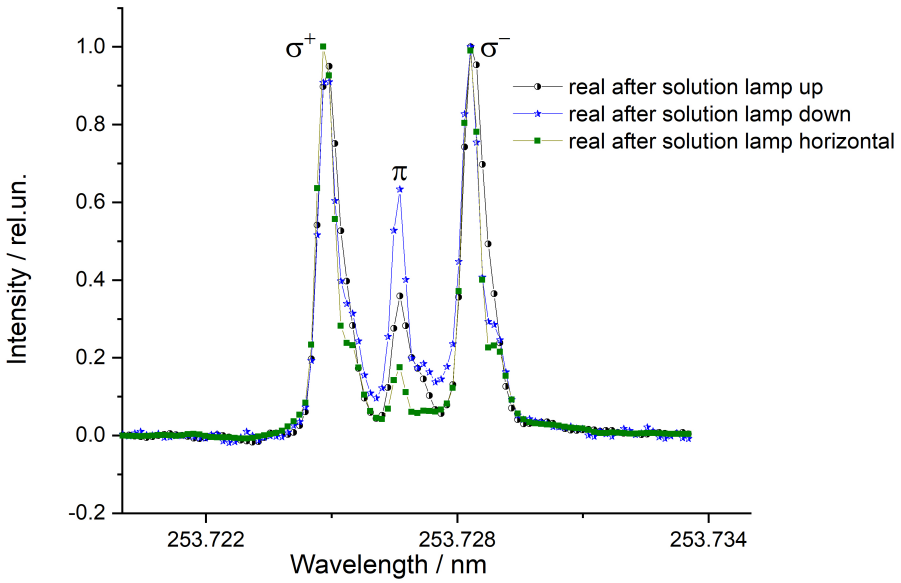

Figure 3. The shapes of the emitted Hg 253.7 nm line, depending on the position of the lamp in a magnetic field.

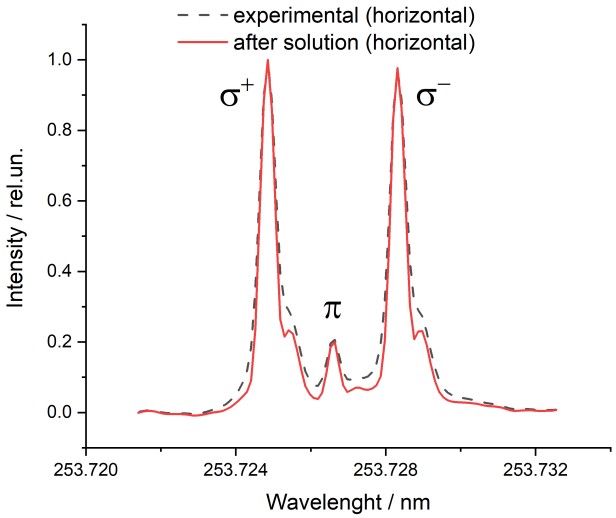

Figure 4. The comparison of the measured Hg 253.7 nm line shape and the "real after solution" one (profile shape after implementation of deconvolution procedure) for horizontal position.

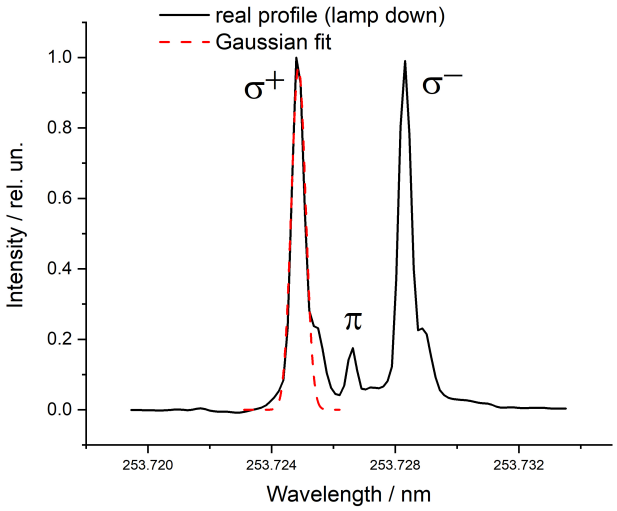

Figure 5. An example of the left σ component Gaussian fit. The calculated FWHM is $(5.42 \pm 0.37) \times 10^{-4}$ *nm with Chi–Square 0.0065 for vertical (lamp down) position.*

In Figure 4 we can see the example of a comparison of the measured Hg 253.7 nm line shape with the "real" Hg 253.7 nm line shape obtained after the solution of the ill–posed task (Equation (1)). The lamp is situated horizontally. Figure 5 shows the "real" Hg 253.7 nm line shape and its Gauss fitting in the same case.

In Table (1) we can see the values of the full width at half of the maximum (FWHM) of 253.7 nm mercury spectral line for three different positions. The values of FWHM of Hg 253.7 nm spectral line were calculated from spectral line profiles after implementing the deconvolution procedure.

As can be seen from Table (1), the FWHM is smaller for horizontally operated capillary, the vertical positions both have similar higher values of the FWHM. The broader emission lines for the vertical positions can be explained by the self–absorption since 253.7 nm is the resonance line.

The cold spot temperature determining the Hg vapour pressure in the lamp in all three positions was quite similar, giving the mercury pressure around 0.005 Torr ($\approx$ 0.7 Pa). This proves that the distribution of atoms has the greatest influence on the broadening of spectral lines.

In general, it agrees with the previous results from tomography of the capillary using visible triplet lines [13]. It was shown that the horizontal position has the most homogeneous radial distribution of emission coefficients, but the vertical position is characterized by a higher level of distribution inhomogeneity, so the emission lines in these cases are more impacted by the self–absorption.

Thus, temperature estimation from the Doppler broadening could be possible only from the horizontal position but still, it can be influenced by the self–absorption, so it can be seen only as a maximum value.

4.2. The dependence of the energy level $^3P_1$ Zeeman splitting on the intensity of magnetic field

Taking into account equations (4) and (6) the dependencies of Zeeman splitting of the energy level $^3P_1$ on the intensity of the magnetic field can be obtained.

The graphs of these dependencies in cases of ^{198}Hg, ^{201a}Hg, ^{201b}Hg, ^{201c}Hg and ^{198}Hg and ^{199a}Hg, ^{199b}Hg are shown in Figures 6 and 7, accordingly.

Considering equation (6), and the value of the energy of the ΔW obtained from the measurements, the value of the magnetic field in our experiment was 3844.8± 6.7 oersteds.

The value of the energy level $^3P_1$ Zeeman splitting was calculated for three working positions of HFEDL and the mean value equals $\Delta W = 0.27\, cm^{-1}$.

5. Conclusions

Diagnostics of line profile is essential when light sources with clearly specified emission line shapes are required. In this paper, the spectral line profiles were deconvoluted, 'real' profile shapes were estimated, and the temperature of plasma was calculated in different working positions of the capillary. Among the investigated capillary operating positions, it was found that the lamp exhibited the lowest optical density when operated horizontally. Hg cold spot temperature was measured for pressure determination. The dependence of Zeeman splitting of energy level $^3P_1$ on the magnetic field was calculated for all stable isotopes of mercury, and the value of the magnetic field in the experiment was accurately determined as well.

Hg 253.7 nm, Capillary operation position	**Real, FWHM average from two σ peaks, nm**	**Temperature, max value, K**
Horizontal	0.000554 ± 0.000009	1840 ± 50
Reservoir up	0.000706 ± 0.000008	2990 ± 70
Reservoir down	0.000717 ± 0.000012	3080 ± 100

Table 1. Full width at half of the maximum and temperature of Hg 253.7 nm spectral line in different working positions

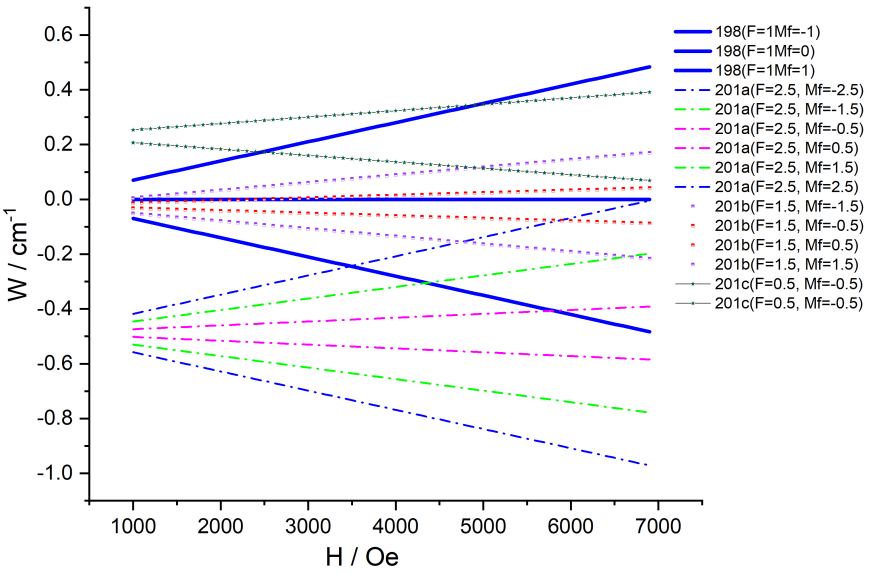

Figure 6. The dependence of Zeeman splitting of energy level $^3P_1$ on the magnetic field for ^{198}Hg, ^{201a}Hg, ^{201b}Hg, and ^{201c}Hg. (Remark: 1 Oe=79.6 A/m)

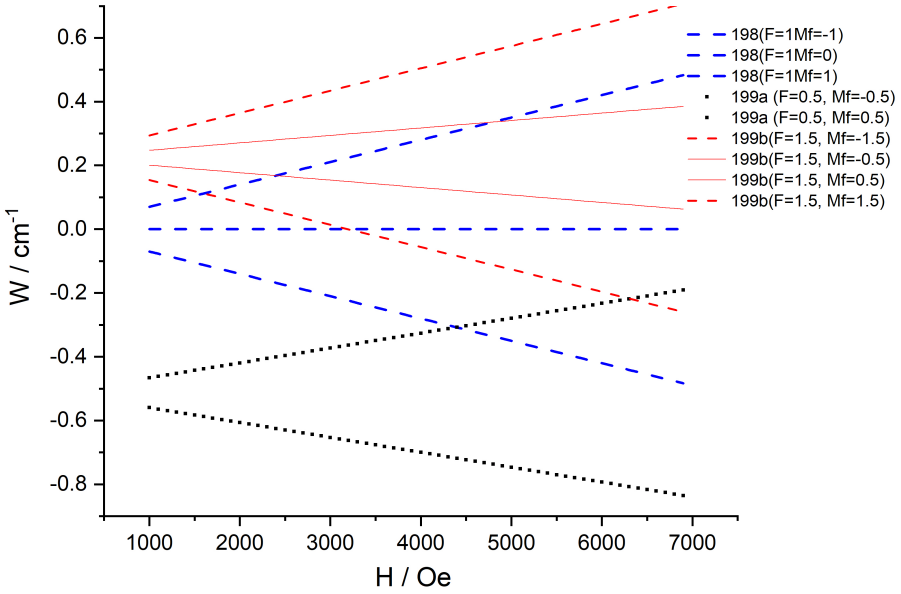

Figure 7. The dependence of Zeeman splitting of the energy level $^3P_1$ on the magnetic field for ^{198}Hg, ^{199a}Hg, and ^{199b}Hg. (Remark: 1 Oe=79.6 A/m)

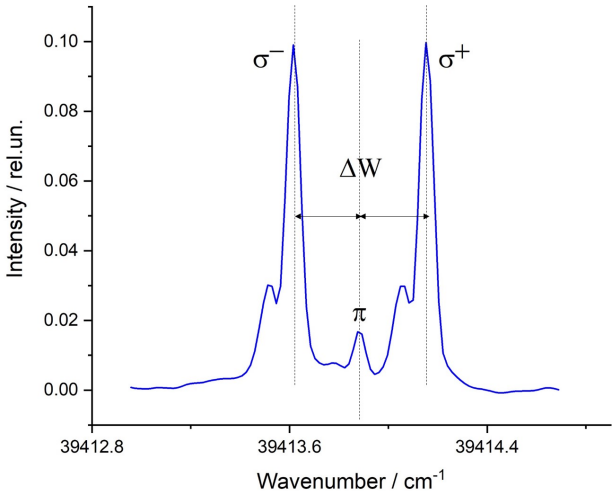

Figure 8. The example of ^{198}Hg for measurements of the energy level $^3P_1$ Zeeman splitting (position of the light source – horizontal).

Acknowledgements

The research was supported by UL IAPS, ERDF "University of Latvia and Institutes in European Research Area - Excellence, Activity, Mobility, Capacity" No. 1.1.1.5/18/I/016, the Latvian Council of Science Project No. lzp–2020/1–0005, and Latvian National State Research Programme project "Smart materials, Photonics, Technologies and Engineering Ecosystem [MOTE]" No. VPP–EM–FOTONIKA–2022/1–0001.

References

[1] A. Ganeev, Z. Gavare, V. I. Khutorshikov, et al. High–frequency electrodeless discharge lamps for atomic absorption analysis. *Spectrochimica Acta Part B: Atomic Spectroscopy*, 58(5):879–889, 2003. doi:10.1016/s0584-8547(03)00020-x.

[2] S. Sholupov and A. Ganeyev. Zeeman atomic absorption spectrometry using high frequency modulated light polarization. *Spectrochimica Acta Part B: Atomic Spectroscopy*, 50(10):1227–1236, 1995. doi:10.1016/0584-8547(95)01316-7.

[3] N. Denisova, E. Bogans, G. Revalde, and J. Skudra. A study of physical processes in microplasma capillary discharges. *The European Physical Journal Applied Physics*, 56(2):24003, 2011. doi:10.1051/epjap/2011110157.

[4] N. Zorina, G. Revalde, and R. Disch. Deconvolution of the mercury 253.7 nm spectral line shape for the use in absorption spectroscopy. In J. Spigulis, A. Krumins, D. Millers, et al., editors, *SPIE Proceedings*. SPIE, 2008. doi:10.1117/12.815460.

[5] W. L. Wiese, D. E. Kelleher, and D. R. Paquette. Detailed study of the stark broadening of balmer lines in a high-density plasma. *Physical Review A*, 6(3):1132–1153, 1972. doi:10.1103/PhysRevA.6.1132.

[6] H. Zhang, C. Hsiech, I. Ishii, et al. Revised, fast, flexible algorithms for determination of electron number densities in plasma discharges. *Spectochimica Acta Part B: Atomic Spectroscopy*, 49(8):817–828, 1994. doi:10.1016/0584-8547(94)80073-1.

[7] G. Revalde, N. Zorina, A. Skudra, and Z. Gavare. Deconvolution of the line spectra of microsize light sources in the magnetic field. *Romanian Reports in Physics*, 66(4):1099–1109, 2014.

[8] N. Zorina, A. Skudra, G. Revalde, and Z. Gavare. Comparison of As, Hg and Tl high-frequency electrodeless lamps for detection of environmental pollution. *ENVIRONMENT. TECHNOLOGIES. RESOURCES. Proceedings of the International Scientific and Practical Conference*, 1:275–280, 2021. doi:10.17770/etr2021vol1.6529.

[9] H. Kopfermann. *Nuclear moments*, volume 16. New York, Academic Press, 1958.

[10] M. Witkowski, G. Kowzan, R. Munoz-Rodriguez, et al. Absolute frequency and isotope shift measurements of mercury $^1S_0 - ^3P_1$ transition. *Optics Express*, 27(8):11069, 2019. doi:10.1364/oe.27.011069.

[11] A. Linek, P. Morzyński, and M. Witkowski. Absolute frequency measurement of the $6s_2^1S_0 \rightarrow 6s6p^3P_1$ $F = 3/2 \rightarrow F' = 5/2$ ^{201}Hg transition with background–free saturation spectroscopy. *Optics Express*, 30(24):44103, 2022. doi:10.1364/oe.475986.

[12] S. Frish. *Optical spectres of atoms*. Gosudarstvennoe izdateljstvo fiziko matematicheskoj literaturi, Russian edition, 1963.

[13] N. Denisova, E. Bogans, G. Revalde, and A. Skudra. Imaging of emitting mercury atom spatial distributions in a capillary discharge lamp by using tomography approach. *IEEE Transactions on Plasma Science*, 36(4):1188–1189, 2008. doi:10.1109/tps.2008.926967.